ACS APPLIED MATERIALS & INTERFACES

Research Article

www.acsami.org

Tuning the Interfacial Thermal Conductance between Polystyrene and Sapphire by Controlling the Interfacial Adhesion

Kun Zheng,[†,§] Fangyuan Sun,[‡] Xia Tian,[‡,∥] Jie Zhu,[*,‡] Yongmei Ma,[*,†] Dawei Tang,[‡] and Fosong Wang[†]

[†]Institute of Chemistry and [‡]Institute of Engineering Thermophysics, Chinese Academy of Sciences, Beijing 100190, P. R. China

[§]University of Chinese Academy of Sciences, Beijing 100049, P. R. China

[∥]Thermal Engineering and Power Department, China University of Petroleum, Qingdao 266580, P. R. China

Supporting Information

ABSTRACT: In polymer-based electric microdevices, thermal transport across polymer/ceramic interface is essential for heat dissipation, which limits the improvement of the device performance and lifetime. In this work, four sets of polystyrene (PS) thin films/sapphire samples were prepared with different interface adhesion values, which was achieved by changing the rotation speeds in the spin-coating process. The interfacial thermal conductance (ITC) between the PS films and the sapphire were measured by time domain thermoreflectance method, and the interfacial adhesion between the PS films and the sapphire, as measured by a scratch tester, was found to increase with the rotation speed from 2000 to 8000 rpm. The ITC shows a similar dependence on the rotation speed, increasing up to a 3-fold from 7.0 ± 1.4 to 21.0 ± 4.2 MW/(m^2 K). This study demonstrates the role of spin-coating rotation speed in thermal transport across the polymer/ceramic interfaces, evoking a much simpler mechanical method for tuning this type of ITC. The findings of enhancement of the ITC of polymer/ceramic interface can shed some light on the thermal management and reliability of macro- and microelectronics, where polymeric and hybrid organic−inorganic nano films are employed.

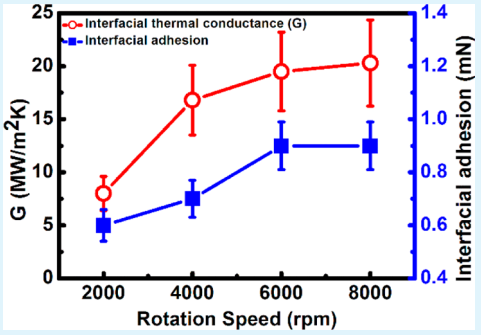

KEYWORDS: *interfacial thermal conductance, interfacial adhesion, spin-coating, polymer thin film, time domain thermoreflectance*

1. INTRODUCTION

Organic and hybrid organic−inorganic materials are promising candidates for next-generation electronic devices because they are low-cost, flexible and lightweight,[1,2] and research on how to engineer the materials for excellent properties, such as thermal conductivity,[3,4] has been carried out. For example, tuning the thermal conductivity of organic and hybrid organic−inorganic materials is now possible by manipulating the chain orientation,[5,6] the chain length,[7] and the interfaces between the organic/inorganic materials.[8] As the characteristic dimension of these structures approach the nanoscale, the role of the interfaces becomes increasingly significant in thermal transport because the interfacial thermal resistance approaches a magnitude similar to that of the material itself.[9,10] The low interfacial thermal conductance (ITC) between polymer and ceramic has been considered one of the bottlenecks for the thermally conductive hybrid nanocomposites that are urgently needed in electronic devices, solid-state lighting, and energy generators.[11−13]

Enhancing either the mechanical or chemical adhesion between the interfaces has been carried out to improve or to understand the nature of thermal transport across the interface. At the metal/inorganic interface, ITC can be improved significantly by introducing a chemically bonded layer.[14,15] For example, transitioning from van der Waals to covalent bonding between gold (Au) and quartz (Qz) via a chemical bonding layer increases the ITC by ∼80% for Au/Qz interfaces.[14] Similarly, using a strong-bonded molecular monolayer at the metal/dielectric interfaces achieves a 4-fold increase of the ITC in the copper−silica system.[15]

At polymer/ceramic interfaces, however, the role of interfacial adhesion on ITC is not clear and only few studies have been carried out to understand the mechanism therein.[16,17] For example, Liu et al.[16] have investigated the ITC between spin-coated polystyrene (PS) films and silicon and found that the ITC increases when the thickness of the PS film is comparable to or smaller than the radius of gyration of bulk PS, which may affect the interfacial adhesion between PS and silicon. However, there have been no experimental data supporting this assumption. Losego et al.[17] have measured the effective thermal conductivity of 1 to 10 nm thick spin-coated poly(methyl methacrylate) (PMMA) films and showed that the effective thermal conductivity is dominated by the bulk thermal conductivity of PMMA when the film thickness is larger than 3 nm, whereas the effective thermal conductivity begins to decrease when the film thickness is below 3 nm because the interfacial thermal resistance between PMMA and its neighboring materials is of the same order of the PMMA thermal resistance itself. Our previous work found that the ITC between spin-coated high density poly-

Received: August 4, 2015
Accepted: October 9, 2015
Published: October 9, 2015

DOI: 10.1021/acsami.5b07188
ACS Appl. Mater. Interfaces 2015, 7, 23644−23649

ethylene (HDPE) films and sapphire decreases with increasing thickness of the HDPE films.[18]

Spin-coating has received great attention over the past two decades for the fabrication of ultrathin functional materials with nanometer level control for various applications, such as low leakage dielectric films, diffusion barrier coatings, transparent conducting coatings, and organic photovoltaic device.[19−21] The spin-coating parameters, such as the environmental temperature and relative humidity, rotation speed, and type of solvents, dominate the interfacial structure between the spin-coated thin film and the substrate.[22,23] Therefore, in addition to the radius of gyration and the thickness of polymer films, the spin-coating parameters should also affect the ITC between polymer films and the substrate in a controllable way.

In this study, we demonstrate a very efficient mechanical method to manipulate and understand thermal transport across the interface between a spin-coated polymer (PS) film and a ceramic (sapphire) substrate, by altering the rotation speed during the spin-coating process. A 3-fold increase of ITC from 7.0 ± 1.4 to 21.0 ± 2.8 MW/(m^2 K) is achieved. Results show that the improvement of the interfacial adhesion is the underlying mechanism for the ITC increase, which can be employed to effectively tune the ITC between the polymer and the ceramic in a mechanical way.

2. MATERIALS AND METHODS

2.1. Materials. The polystyrene (M_w: 65 000 g/mol and M_w/M_n = 1.06) was purchased from Alfa and the radius of gyration of the bulk polystyrene coil (R_g) was 7.1 nm, which was calculated by $R_g = 0.028\sqrt{M}$ (nm).[24] The sapphires (0001) were supplied by Hefei Kejing Materials Technology CO., LTD, with dimensions of 1 cm × 1 cm × 400 μm and the surface roughness is less than 0.4 nm.

2.2. PS Film Preparation. Four sets of polystyrene (PS) films on sapphire with various levels of interfacial adhesion were prepared by spin-coating with rotation speeds of 2000, 4000, 6000, and 8000 rpm. The PS was dissolved in toluene (>99.9%) at concentrations of 1.4, 1.6, 1.7, and 1.8 wt % to prepare films with different thicknesses at a set rotation speed.

2.3. Characterization. *2.3.1. Surface Morphology Measurement.* The surface roughness (R_a) of the prepared PS thin films was characterized by tapping-mode atomic force microscopy (AFM), Bruker Nanoscope V Multimode 8.

2.3.2. Thickness of PS Film Measurement. Thickness measurements for the PS films using a spectroscopic ellipsometer (M-2000 V, J. A. Woollam) were conducted at an incidence angle of 70° and a wavelength scan from 370.1−999.1 nm.[25] In this study, the well-established Cauchy dispersion model was used to fit the ellipsometry data[26] because no absorption of incident light exists for all of the samples under investigation. By this model, the refractive index of the substances follows the relation of $r = A+(B/\lambda^2)$, where r is the refractive index, λ is the wavelength of the probing light, and A and B are two fitting parameters related to r. For the thickness measurements, B was set at 0.01 and A was set at 1.60 for the PS films.[25]

2.3.3. Scratch Test. Interfacial adhesion between the PS film and the sapphire were measured using CSM nano scratch tester in ambient air, at the temperature of 23 °C and a humidity of 20%.[27,28] At least three identical scratches were produced on each specimen using the same test parameters consisting of a Rockwell diamond indenter (stylus type), a 2 μm stylus radius, a 0.3 initial load mN, a 2 mN end load, a 50 μm scratch length, and a 50 μm/min stylus velocity. Specifically, the diamond indenter was drawn across the PS film under an increasing continuous load until at a certain load, termed as the critical load, L_c, a well-defined failure event occurred. If this failure event was a coating detachment, the critical load could then be used as a qualitative measure of the coating-substrate interfacial adhesion.[29,30]

2.3.4. Interfacial Thermal Conductance Measurement. The ITC between PS thin films and sapphire was measured using the time domain thermoreflectance (TDTR) method, which is a well-accepted optical measurement technique for characterizing thermal properties of bulk and thin film materials. The reader may refer to Figure S1 for more detailed information about the experimental setup.[18,31−34] Prior to ITC measurement, an ∼100 nm thick Al thin film transducer was prepared on the spin-coated PS thin films by electron beam evaporation,[15,20] which serves as both a heater that absorbs the pump laser beam and as a thermometer where the temperature-induced reflectivity change was measured through the probe laser beam. The sample structure can be found in Figure S2. The detected thermal response from the surface of the Al thin film is then fitted with a heat transfer model to extract the unknown thermal properties of materials, such as the ITC between PS film and sapphire substrate (more details can be found in the Supporting Information).

3. RESULTS AND DISCUSSION

3.1. Thickness of PS Films. Figure 1 shows that the thickness of the PS films decreases with increased rotation speed

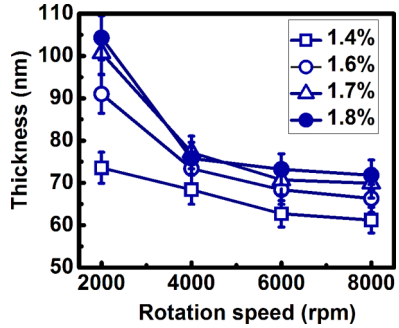

Figure 1. Thickness of PS films as a function of rotation speeds during spin-coating process from 2000 to 8000 rpm at four concentrations from 1.4 to 1.8 wt %.

at all concentrations,[22] where the thickness of the PS films decreases sharply when the rotation speed increase from 2000 to 4000 rpm and then become almost stable when the rotation speed exceeds 6000 rpm.[22] This observation can be explained by the presence of two competing mechanisms in the spin-coating process. In the initial few seconds, the convection of fluid in the radial direction accompanied by rapid thinning dominates the process, whereas later in the process, the convection becomes negligible and the process is dominated by the evaporation of the solvent controlled by diffusion.[35] When the rotation speed is less than 4000 rpm in this process, the film thinning occurs mainly during the initial period, which gives rise to a remarkable change of film thickness in a range around this rotation speed.

3.2. Morphology of PS Films. Figure 2 shows the surface morphologies of the PS films prepared with different rotation speeds. It can be seen that the morphologies of the films appear similar and the surfaces are very smooth with a roughness of less than 0.5 nm,[36,37] which satisfies the TDTR measurement requirement for acquiring reliable signals. The rotation speed seems to have a negligible effect upon on the surface morphology of the PS film, which also reduces the uncertainty caused by the surface roughness for thermal property measurements.[38]

3.3. Interfacial Adhesion. It is well-known that applying enhanced pressure on films can increase the adhesion between the films and their substrates. However, to change the adhesion between a nanofilm and the substrate is challenging because applying a force directly on the film increases the risk of film damage. Here, we prepared samples with different interfacial adhesion by changing the spin parameters (rotation speed)

DOI: 10.1021/acsami.5b07188
ACS Appl. Mater. Interfaces 2015, 7, 23644−23649

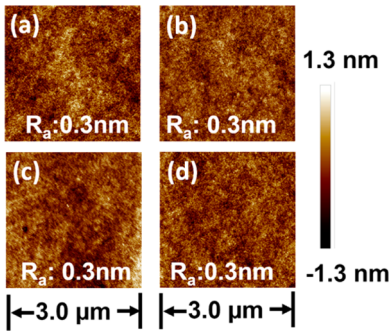

Figure 2. AFM image of surface structure of PS films; a−d represents rotation speed 2000, 4000, 6000, and 8000 rpm, respectively. R_a represents the surface roughness.

during coating process. The interfacial adhesion between the PS films and the sapphire substrates was measured using a nano scratch tester in ambient air, at a temperature of 23 °C and a humidity of 20% (see Section 2.3.3 in Materials and Method).[27,28] In terms of the critical load, the interfacial adhesion can be influenced by many factors, such as the thickness and roughness of the films.[39] In this work, the roughness and thicknesses of the PS films used for interfacial adhesion measurements are 0.5 ± 0.1 and 70 ± 2 nm, respectively, where the relatively small uncertainties ensure the accuracy of the entire experiment. As shown in Figure 3, the interfacial adhesion between PS films and sapphire increases from 0.6 ± 0.12 mN at 2000 rpm to 0.9 ± 0.18 mN at 6000 and 8000 rpm.

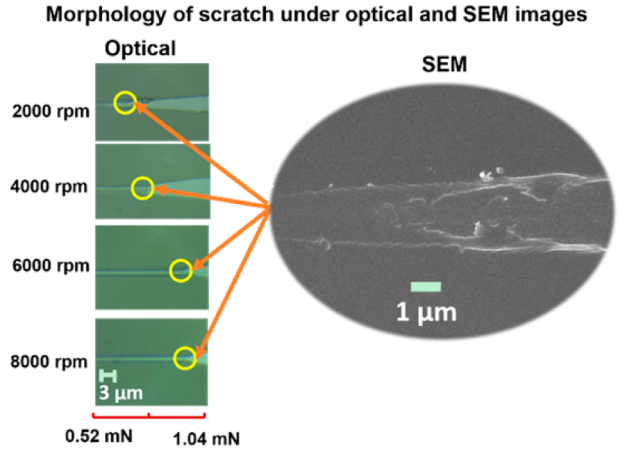

Figure 3. Interfacial test under optical and SEM image. The yellow circles under optical image are where the delamination occurs, as observed from the SEM image.

3.4. Interfacial Thermal Conductance between PS and Sapphire. The ITC between PS thin films and sapphire substrates was measured using the time domain thermoreflectance (TDTR) method, which is a well-accepted thermal property characterization technique for bulk and thin film materials.[18,31−34] The thermal penetration depth is greater than 200 nm, which guarantees that the thermal wave will reach the interface, and further information about the thermal penetration can be found in Figure S3. We calibrated our TDTR system by measuring many standard samples, such as, silicon, silicon dioxide and sapphire prior to measuring the unknown samples. The refractive indices of all of the PS films fall in a narrow range (Figure S5), which means the bulk density maintained even with the varying thicknesses of the films. Three scans were taken and averaged for each sample to reduce the measurement uncertainty and relatively thicker PS samples (172 nm) were measured for calibration, whose fitted value of the PS thermal conductivity and Al/PS interfacial thermal conductance are 0.15 ± 0.01 W/(m K) and 20.0 ± 4.0 MW/(m^2 K), respectively, which agrees with the results of Liu et al.[16] Additionally, the ITC between Al and PS has been reported to be independent of the PS film thickness,[16] which means that the ITC between the spin-coated PS and the sapphire is the only unknown parameter in the data fitting process. Figure 4 shows the TDTR signals of samples prepared

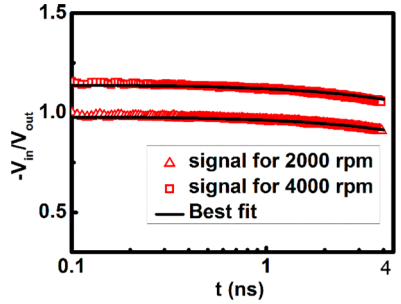

Figure 4. TDTR signals of $-V_{in}/V_{out}$ and the corresponding best fit to the theoretical thermal model of the PS films with thicknesses 73.6 and 73.4 nm prepared by 2000 and 4000 rpm, respectively.

with a rotation speed of 2000 and 4000 rpm and the corresponding best fit curves to the heat transfer model (see the Supporting Information for more information).

Figure 5 plots the measured ITC between PS films and sapphire as a function of the rotation speed at a thickness of ∼70

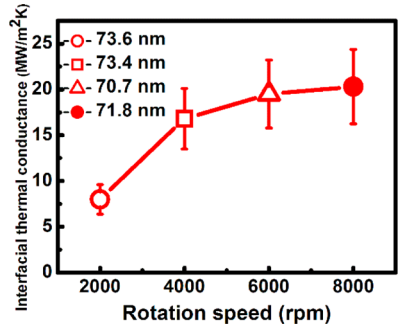

Figure 5. Interfacial thermal conductance between PS film and sapphire increases with rotation speed.

nm. As shown in Figure 5, the ITC increases approximately 3-fold, from 7.0 ± 1.4 to 21.0 ± 4.2 MW/(m^2 K), with a rotation speed increase from 2000 to 8000 rpm. Our measurement results for the ITC between PS thin films and neighboring materials are in reasonable agreement with previous measurements (PS/Si interface, 8−16 MW/(m^2 K);[16] HDPE/sapphire, 8 MW/(m^2 K)[18]) and with simulation (amorphous polyethylene/Si interface, 20 MW/(m^2 K)[40]).

To rule out the effects of the PS film thickness upon the ITC, we plotted the relationship between the thickness and the ITC in Figure 6. Here, the ITC value remains constant at the identical rotation speeds for thicknesses changing from ∼60 to ∼100 nm. In this scenario, the radius of gyration of PS, around 7.1 nm,[24] is much smaller than these film thicknesses exceeding 60 nm and we postulate that the main chain conformation in our PS films is

DOI: 10.1021/acsami.5b07188
ACS Appl. Mater. Interfaces 2015, 7, 23644−23649

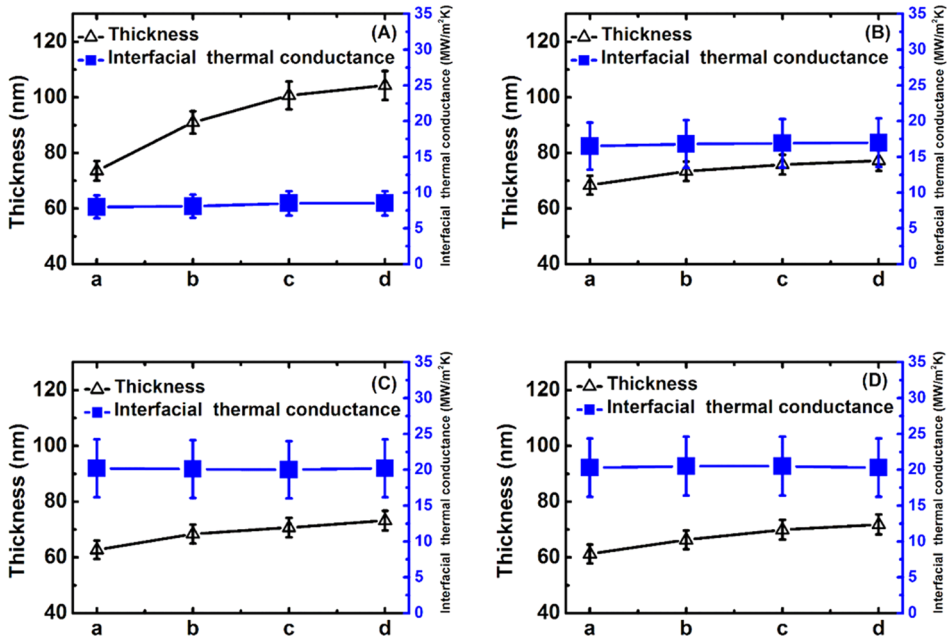

Figure 6. Film thickness (left axis) and interfacial thermal conductance between PS film and sapphire substrate (right axis) as a function of the concentration of the spin-coating process at rotation speed: (A) 2000 rpm, (B) 4000 rpm, (C) 6000 rpm, and (D) 8000 rpm; a–d represent concentration of PS in toluene, which are 1.4, 1.6, 1.7, and 1.8 wt %, respectively.

approximately the same as that in bulk PS because the chain structure is similar to the counterpart bulk material when the film thickness is greater than five times the radius of gyration.[41,42] According to Liu et al.,[16] when the thickness of the PS film is much greater than the radius of gyration, the ITC is not affected by the thickness. These results, however, contradict those of Losego et al.[17] using PMMA and our previous paper using HDPE[18] and this interesting phenomenon can possibly be attributed to the following aspects.

First, the thermal properties may depend upon a length scale typically from several to hundreds of nanometers. In the research of Losego et al., the effective thermal conductivity begins to decrease when the film thickness is less than 3 nm, but in our case the film is thicker than 60 nm, which suggests a different story.

Second, the structure of the HDPE film can change substantially at different thicknesses because it is a polymer possessing a high crystallinity and a complex crystal type.[43] Nevertheless, the PS used in this study is amorphous, and therefore possesses a film structure that is totally different from HDPE films, which may also produce the different trend in the ITC.

These differing ITC trend are an interesting issue, and the underlying mechanism could be further studied in the future with much more data of ITC between polymer and dielectric materials.

In this work, therefore, it is reasonable to conclude that the ITC is practically constant for spin-coated films of varying thickness deposited at the same rotation speed, which confirms that the ITC is affected by rotation speed.

It is also should be noted that the ITC increases rapidly from 7.0 ± 1.4 to 16.0 ± 3.2 MW/(m^2 K) with increasing rotation speed from 2000 to 4000 rpm, which then levels off at a value of ~20 MW/(m^2 K) at higher rotation speeds. This behavior can be explained by the possibility that the polymer chain conformation near the interface is formed in the initial few seconds and then is rapidly frozen because of the rapid solvent evaporation caused by the substrate rotation,[44−46] which then dominates the interfacial adhesion. In other words, when the rotation speed exceeds a critical speed, the interfacial adhesion can only be slightly affected by increasing the speed further because the solvent evaporation reaches a constant value. As shown in Figure 7, the ITC can be

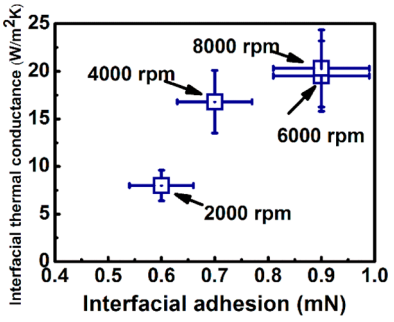

Figure 7. Interfacial thermal conductance between PS film and sapphire substrate as a function of interfacial adhesion.

tuned predominantly by rotation speed when it is lower than the critical rotation speed (4000 rpm in our case), which shows a trend similar to that of the interfacial adhesion. It is obvious that the ITC increases with increasing interfacial adhesion, which is in agreement with metal/inorganic interfaces.[14,15]

4. CONCLUSIONS

We have experimentally shown that the rotation speed of the spin-coating process plays an important role in the ITC between PS and sapphire. Specifically, the ITC gained a 3-fold increase from 7.0 ± 1.4 to 21.0 ± 4.2 MW/(m^2 K) with the rotation speed increasing from 2000 to 8000 rpm. We also verified that under a constant rotation speed condition, when the film thickness is much larger than the PS gyration radius, the ITC is not affected by the film thickness. The scratch test verified that the enhancement of ITC was owing to the increase of the interfacial adhesion increasing. These results show that in multilayered

DOI: 10.1021/acsami.5b07188
ACS Appl. Mater. Interfaces 2015, 7, 23644−23649

materials fabricated by spin-coating, the rotation speed plays an essential role in thermal transport across the interfaces, which provides a simple and effective way to mechanically tune the ITC between polymer and ceramic and suggests the potential for further studies to better understand the phenomenon. Our method to improve ITC of polymer/ceramic interfaces can shed some light on the thermal management and reliability of macro- and microelectronics, where polymeric and hybrid organic–inorganic nano films are employed.

■ ASSOCIATED CONTENT

Supporting Information

The Supporting Information is available free of charge on the ACS Publications website at DOI: 10.1021/acsami.5b07188.

Brief description of TDTR measurement and the refractive index data (PDF)

■ AUTHOR INFORMATION

Corresponding Authors

*E-mail: zhujie@iet.cn. Tel: 86-10-82543022. Fax: 86-10-82543022.

*E-mail: maym@iccas.ac.cn. Tel: 86-10-62659019. Fax: 86-10-62532144.

Notes

The authors declare no competing financial interest.

■ ACKNOWLEDGMENTS

This work was supported by the National Natural Science Foundation of China (Grant Nos. 51373184 and 51336009), the National Plan for Science & Technology Support, China (Grant No. 2014BAC03B05), and the MoST (Ministry of Science and Technology) 973 Research Programme (Grant Nos. 2014CB931803 and 2012CB933801).

■ REFERENCES

(1) Judeinstein, P.; Sanchez, C. Hybrid Organic–Inorganic Materials: a Land of Multidisciplinarity. *J. Mater. Chem.* **1996**, *6*, 511–525.

(2) Chujo, Y. Organic-Inorganic Hybrid Materials. *Curr. Opin. Solid State Mater. Sci.* **1996**, *1*, 806–811.

(3) Soles, C. L.; Ding, Y. Nanoscale Polymer Processing. *Science* **2008**, *322*, 689–690.

(4) Liu, J.; Yoon, B.; Kuhlmann, E.; Tian, M.; Zhu, J.; George, S. M.; Lee, Y.-C.; Yang, R. Ultralow Thermal Conductivity of Atomic/Molecular Layer-Deposited Hybrid Organic–Inorganic Zincone Thin Films. *Nano Lett.* **2013**, *13*, 5594–5599.

(5) Shen, S.; Henry, A.; Tong, J.; Zheng, R.; Chen, G. Polyethylene Nanofibres with Very High Thermal Conductivities. *Nat. Nanotechnol.* **2010**, *5*, 251–255.

(6) Kurabayashi, K.; Goodson, K. E. Impact of Molecular Orientation on Thermal Conduction in Spin-Coated Polyimide Films. *J. Appl. Phys.* **1999**, *86*, 1925–1931.

(7) Liu, J.; Yang, R. Length-Dependent Thermal Conductivity of Single Extended Polymer Chains. *Phys. Rev. B: Condens. Matter Mater. Phys.* **2012**, *86*, 104307.

(8) Liu, J.; Alhashme, M.; Yang, R. Thermal Transport Across Carbon Nanotubes Connected by Molecular Linkers. *Carbon* **2012**, *50*, 1063–1070.

(9) Luo, T.; Chen, G. Nanoscale Heat Transfer–from Computation to Experiment. *Phys. Chem. Chem. Phys.* **2013**, *15*, 3389–3412.

(10) Cahill, D. G.; Ford, W. K.; Goodson, K. E.; Mahan, G. D.; Majumdar, A.; Maris, H. J.; Merlin, R.; Phillpot, S. R. Nanoscale Thermal Transport. *J. Appl. Phys.* **2003**, *93*, 793–818.

(11) Pop, E. Energy Dissipation and Transport in Nanoscale Devices. *Nano Res.* **2010**, *3*, 147–169.

(12) Gong, F.; Bui, K.; Papavassiliou, D. V.; Duong, H. M. Thermal Transport Phenomena and Limitations in Heterogeneous Polymer Composites Containing Carbon Nanotubes and Inorganic Nanoparticles. *Carbon* **2014**, *78*, 305–316.

(13) Hung, M.-T.; Choi, O.; Ju, Y. S.; Hahn, H. Heat Conduction in Graphite-Nanoplatelet-Reinforced Polymer Nanocomposites. *Appl. Phys. Lett.* **2006**, *89*, 023117.

(14) Losego, M. D.; Grady, M. E.; Sottos, N. R.; Cahill, D. G.; Braun, P. V. Effects of Chemical Bonding on Heat Transport Across Interfaces. *Nat. Mater.* **2012**, *11*, 502–506.

(15) O'Brien, P. J.; Shenogin, S.; Liu, J.; Chow, P. K.; Laurencin, D.; Mutin, P. H.; Yamaguchi, M.; Keblinski, P.; Ramanath, G. Bonding-Induced Thermal Conductance Enhancement at Inorganic Heterointerfaces Using Nanomolecular Monolayers. *Nat. Mater.* **2013**, *12*, 118–122.

(16) Liu, J.; Ju, S.; Ding, Y.; Yang, R. Size Effect on the Thermal Conductivity of Ultrathin Polystyrene Films. *Appl. Phys. Lett.* **2014**, *104*, 153110.

(17) Losego, M. D.; Moh, L.; Arpin, K. A.; Cahill, D. G.; Braun, P. V. Interfacial Thermal Conductance in Spun-Cast Polymer Films and Polymer Brushes. *Appl. Phys. Lett.* **2010**, *97*, 011908.

(18) Zheng, K.; Zhu, J.; Ma, Y.; Tang, D.; Wang, F. Interfacial Thermal Resistance Between High-Density Polyethylene (HDPE) and Sapphire. *Chin. Phys. B* **2014**, *23*, 107307.

(19) Chang, C. C.; Pai, C. L.; Chen, W. C.; Jenekhe, S. A. Spin Coating of Conjugated Polymers for Electronic and Photoelectronic Applications. *Thin Solid Films* **2005**, *479*, 254–260.

(20) Duda, J. C.; Hopkins, P. E.; Shen, Y.; Gupta, M. C. Thermal Transport in Organic Semiconducting Polymers. *Appl. Phys. Lett.* **2013**, *102*, 251912.

(21) Wang, Y.; Acton, O.; Ting, G.; Weidner, T.; Shamberge, P. J.; Ma, H.; Ohuchi, F. S.; Castner, D. G.; Jen, A. K. Y. Effect of the Phenyl Ring Orientation in the Polystyrene Buffer Layer on the Performance of Pentacene Thin-Film Transistors. *Org. Electron.* **2010**, *11*, 1066–1073.

(22) Hall, D. B.; Underhill, P.; Torkelson, J. M. Spin Coating of Thin and Ultrathin Polymer Films. *Polym. Eng. Sci.* **1998**, *38*, 2039–2045.

(23) Hou, L. T.; Wang, E.; Bergqvist, J.; Andersson, B. V.; Wang, Z. Q.; Muller, C.; Campoy-Quiles, M.; Andersson, M. R.; Zhang, F. L.; Inganas, O. Lateral Phase Separation Gradients in Spin-Coated Thin Films of High-Performance Polymer: Fullerene Photovoltaic Blends. *Adv. Funct. Mater.* **2011**, *21*, 3169–3175.

(24) DeMaggio, G.; Frieze, W.; Gidley, D.; Zhu, M.; Hristov, H.; Yee, A. Interface and Surface Effects on the Glass Transition in Thin Polystyrene Films. *Phys. Rev. Lett.* **1997**, *78*, 1524–1527.

(25) Chu, X.; Yang, J.; Liu, G.; Zhao, J. Swelling Enhancement of Polyelectrolyte Brushes Induced by External Ions. *Soft Matter* **2014**, *10*, 5568–5578.

(26) Fujiwara, H. *Spectroscopic Ellisometry Principles and Applications*; Maruzen Co.: Tokyo, 2003.

(27) Benjamin, P.; Weaver, C. Measurement of Adhesion of Thin Films. *Proc. R. Soc. London, Ser. A* **1960**, *254*, 163–176.

(28) Chen, Z. X.; Zhou, K.; Lu, X. H.; Lam, Y. C. A Review on the Mechanical Methods for Evaluating Coating Adhesion. *Acta. Mech.* **2014**, *225*, 431–452.

(29) Bull, S. J. Failure Mode Maps in the Thin Film Scratch Adhesion Test. *Tribol. Int.* **1997**, *30*, 491–498.

(30) Wirasate, S.; Boerio, F. J. Effect of Adhesion, Film Thickness, and Substrate Hardness on the Scratch Behavior of Poly(Carbonate) Films. *J. Adhes.* **2005**, *81*, 509–528.

(31) Cahill, D. G.; Watanabe, F. Thermal Conductivity of Isotopically Pure and Ge-Doped Si Epitaxial Layers From 300 to 550 K. *Phys. Rev. B: Condens. Matter Mater. Phys.* **2004**, *70*, 235322.

(32) Zhu, J.; Tang, D.; Wang, W.; Liu, J.; Holub, K. W.; Yang, R. Ultrafast Thermaoreflectance Techniques for Measuring Thermal Conductivity and Interface Thermal Conductance of Thin Films. *J. Appl. Phys.* **2010**, *108*, 094315.

(33) Costescu, R. M.; Wall, M. A.; Cahill, D. G. Thermal Conductance of Epitaxial Interfaces. *Phys. Rev. B: Condens. Matter Mater. Phys.* **2003**, *67*, 054302.

DOI: 10.1021/acsami.5b07188
ACS Appl. Mater. Interfaces 2015, 7, 23644–23649

(34) Capinski, W.; Maris, H.; Ruf, T.; Cardona, M.; Ploog, K.; Katzer, D. Thermal-Conductivity Measurements of GaAs/AlAs Superlattices Using a Picosecond Optical Pump-and-Probe Technique. *Phys. Rev. B: Condens. Matter Mater. Phys.* **1999**, *59*, 8105.
(35) Münch, A.; Please, C. P.; Wagner, B. Spin Coating of an Evaporating Polymer Solution. *Phys. Fluids* **2011**, *23*, 102101.
(36) Housmans, C.; Sferrazza, M.; Napolitano, S. Kinetics of Irreversible Chain Adsorption. *Macromolecules* **2014**, *47*, 3390−3393.
(37) Glynos, E.; Frieberg, B.; Green, P. Wetting of a Multiarm Star-Shaped Molecule. *Phys. Rev. Lett.* **2011**, *107*, 118303.
(38) Hopkins, P. E.; Phinney, L. M.; Serrano, J. R.; Beechem, T. E. Effects of Surface Roughness and Oxide Layer on the Thermal Boundary Conductance at Aluminum/Silicon Interfaces. *Phys. Rev. B: Condens. Matter* **2010**, *82*, 313−319.
(39) Wong, J. S. S.; Sue, H. J.; Zeng, K. Y.; Li, R. K. Y.; Mai, Y. W. Scratch Damage of Polymers in Nanoscale. *Acta Mater.* **2004**, *52*, 431−443.
(40) Hu, M.; Shenogin, S.; Keblinski, P. Molecular Dynamics Simulation of Interfacial Thermal Conductance between Silicon and Amorphous Polyethylene. *Appl. Phys. Lett.* **2007**, *91*, 241910.
(41) Ennis, D.; Betz, H.; Ade, H. Direct Spincasting of Polystyrene Thin Films onto Poly (Methyl Methacrylate). *J. Polym. Sci., Part B: Polym. Phys.* **2006**, *44*, 3234−3244.
(42) Mukhopadhyay, M. K.; Jiao, X.; Lurio, L. B.; Jiang, Z.; Stark, J.; Sprung, M.; Narayanan, S.; Sandy, A. R.; Sinha, S. K. Thickness Induced Structural Changes in Polystyrene Films. *Phys. Rev. Lett.* **2008**, *101*, 115501.
(43) Wang, J.; Lu, G. H.; Li, L. G.; Lu, Z. H.; Yang, X. N.; Zhou, E. L. Novel Morphology of Polyethylene Crystals Created upon Melt Crystallization of Spin-Coated Film. *Macromolecules* **2008**, *41*, 1273−1280.
(44) Lu, X. L.; Myers, J. N.; Chen, Z. Molecular Ordering of Phenyl Groups at the Buried Polystyrene/Metal Interface. *Langmuir* **2014**, *30*, 9418−9422.
(45) Tsuruta, H.; Fujii, Y.; Kai, N.; Kataoka, H.; Ishizone, T.; Doi, M.; Morita, H.; Tanaka, K. Local Conformation and Relaxation of Polystyrene at Substrate Interface. *Macromolecules* **2012**, *45*, 4643−4649.
(46) Chang, L. P.; Morawetz, H. Study of the Interpenetration of Monodisperse Polystyrene in Semidilute Solution by Fluorescence after Freeze-Drying. *Macromolecules* **1987**, *20*, 428−431.

DOI: 10.1021/acsami.5b07188
ACS Appl. Mater. Interfaces 2015, 7, 23644−23649